RADBOUD UNIVERSITY NIJMEGEN

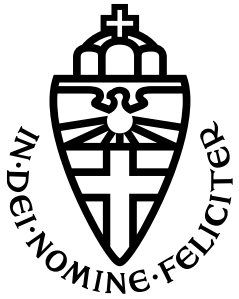

FACULTY OF SCIENCE

HIGH ENERGY PHYSICS

Determination of characteristics of the GRAND antenna setup

Bachelor's Thesis

Author: Bram Ruiter

Supervisor: prof. dr. C.W.J.P. Timmermans

August 17, 2022

Abstract

The Giant Radio Array for Neutrino Detection (GRAND) is a proposed project which aims to measure air showers indirectly initiated by neutrinos. In this thesis the working principles behind the GRAND antenna setup and its characteristics are discussed. Experiments in a lab are used to confirm that the equipment works as expected. A complete installation is used for further confirmation and as a preparation for a larger experiment at the Nançay radio observatory. At this observatory antennas are installed with the aim to detect air showers. Presently, no air showers have been detected yet due to some technical issues.

Contents

1 Introduction

In 2012 CERN's Large Hadron Collider first reached collisions with energies exceeding 10^{12} eV[1]. These high energy particles are crucial for our understanding of fundamental physics in these high energy regimes. However, as you are reading this thesis there are even more highly energetic charged particles entering the Earth's atmosphere, cosmic rays. Some of these cosmic rays have ultra high energies exceeding 10^{18} eV. Thus, these ultra-high-energy cosmic rays (UHECRs) have energies which far exceeds the acceleration capacity of the current man made particle accelerators [1].

UHECRs are likely accelerated by yet unknown cosmic accelerators . Discovering the origin of these highly energetic particles can extend our understanding of fundamental physics to new regimes. To identify the creation mechanisms of these highly energetic particles, the path to the origin must be traced, and the type and energy of the particles must be determined. Cosmic rays can be measured using various methods. The Giant Radio Array for Neutrino Detection (GRAND) is a project which will use radio antennas to directly detect UHECRs and to indirectly detect neutrinos created by UHECRs [1].

In this thesis the characteristics of the antenna setup that will be used in GRAND are determined. Some experiments in a lab are performed to confirm the setup works as it should. Secondly, the complete setup is installed as a preparation for a larger experiment. Lastly, a 3 antenna setup is installed at the Nançay radio observatory with the aim to detect cosmic rays. In section 2 the theory behind the detection principle is explained. Section 3 explains the fundamentals of antennas. The workings of the GRAND antenna setup are explained in section 4. The performed experiments and their results are discussed from section 5 onwards.

[1] `https://home.cern/resources/faqs/facts-and-figures-about-lhc`

2 Cosmic rays

Millions of charged particles are entering the Earth's atmosphere everyday. These charged particles, also called cosmic rays, are created and accelerated by extraterrestrial sources [2]. Some of these cosmic rays have energies up to 10^{20} eV, far exceeding the capabilities of man made particle accelerators. This makes these cosmic rays especially interesting to study. The acceleration mechanisms of these highly energetic cosmic rays are not very well known. To be able to say something useful about the creation mechanisms of these cosmic rays, the energy, particle type and direction of the incoming cosmic rays needs to be determined [1].

2.1 Energy spectrum

The energy spectrum of the incident cosmic rays varies from a few GeV up to 10^{20} eV [2]. Cosmic rays with an energy exceeding 10^{18} eV are called ultra-high-energy cosmic rays (UHECRs). While it is possible to detect cosmic rays with high energies, it is significantly more probable to detect cosmic rays with lower energies. This is because the differential flux[2] decreases as the energy of the cosmic rays increase, meaning highly energetic cosmic rays are more rare. In fact, the relation between the differential flux J and energy E of cosmic rays can be approximated by a power law:

$$J \propto E^{-\gamma} \tag{2.1}$$

where γ is the energy-dependent spectral index with a value close to 3 [2]. In figure 2.1 the measured cosmic ray energy spectrum is plotted, along with the power law described by equation 2.1.

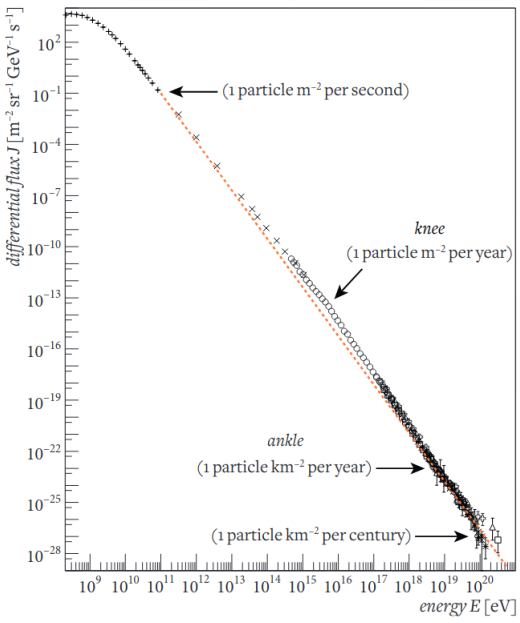

Figure 2.1: The measured cosmic ray energy spectrum. The dashed line corresponds to a linear fit on the logarithmic scale. Figure from [2].

[2]The amount of incident particles per unit area, time and energy.

Cosmic rays can be detected directly using particle detectors, usually placed on high altitudes to limit interactions of cosmic rays with molecules in the atmosphere. The particles which are particularly interesting to measure are those with an ultra high energy ($E \geq 10^{18}$eV). However, as shown in figure 2.1, the differential flux for these particles is extremely low, there are just a few incident particles per km^2 per year. It is practically impossible to directly measure UHECRs, huge detectors are needed just to measure a few particles. In order to measure these ultra-high-energy cosmic rays a different strategy is needed.

2.2 Air showers

As a cosmic ray propagates through the atmosphere, it has a chance to collide with an atmospheric nucleus. During such collisions additional particles are created. These extra particles can also collide with atmospheric nuclei, leading to the creation of even more particles. In this way the cosmic ray initiates a chain reaction in which at each step collisions lead to additional particles. This cascade of reactions leads to millions of particles traveling towards the Earth's surface: an air shower [1]. After a certain amount of collisions the particles in the air shower have too little energy to create additional particles, at this point the air shower will die out [2]. An air shower emits radio waves, this provides a possible measurement tool [1, 2].

In figure 2.2 a schematic overview is given of the evolution of an air shower as it propagates through the atmosphere. There are various particles that can be created in collisions. These particles can be divided into three categories: electromagnetic[3], muonic and hadronic [2]. However, as the air shower propagates through the atmosphere, the contribution of the electromagnetic component to the total energy increases. This is shown schematically in figure 2.2 by the size of the components. The electromagnetic component carries the majority of the total energy of the air shower. By measuring this energy contribution it is possible to determine the energy of the original particle, albeit with some inaccuracy [1].

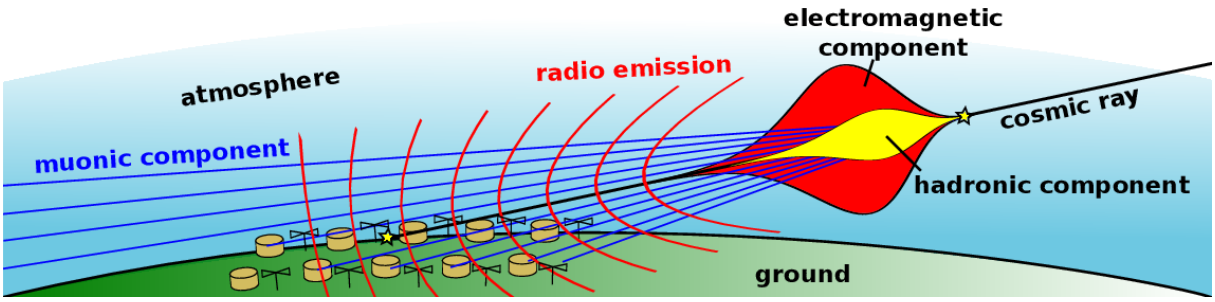

Figure 2.2: Schematic view of an air shower. The width perpendicular to the shower axis denotes the amount of particles in the component. Figure from [3].

[3] electrons, positrons and photons

2.2.1 Shape

The shape of an air shower is determined by its interactions with atmospheric nuclei. A particle has a higher chance to interact if the density of the medium is higher. Since the density of the atmosphere changes as an air shower propagates through the atmosphere, it does not make sense to characterize an air shower by the distance it travelled. Instead, it makes more sense to characterize air showers by the atmospheric depth X, which is a measure of the total traversed mass of the atmosphere[4].

$$X(h) = \int_h^\infty \rho(h')dh' \tag{2.2}$$

The atmospheric depth is measured from the top of the atmosphere and is defined by equation 2.2, where h is the corresponding vertical height, and ρ is the density of the air [2]. This integral is calculated along the propagation direction of the air shower.

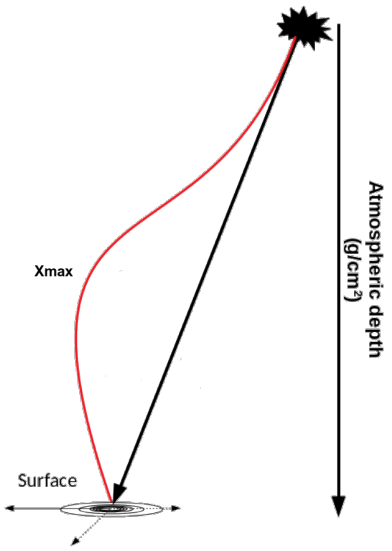

Figure 2.3: A schematic picture of an air shower as it propagates through the atmosphere. The width corresponds to the amount of particles in the air shower. X_{max} is the atmospheric depth at which the amount of particles is at a maximum. Adapted from [4].

The shape of an air shower can be described by the amount of particles in the shower. In a collision, it is likely that additional particles are created if the energy of the incident particle is sufficiently high: $E \geq E_c$ [2]. This means that in early stages of the air shower, every collision is likely to increase the amount of particles N due to the high amount of energy of the cosmic ray that initiated the air shower. After each collision the energy per particle decreases, both because the number of particles increases, but also because energy gets transferred to the air. This means that the amount of particles created at every step decreases. After a certain amount of collisions the energy per particle drops below the critical value $E < E_c$, it is then highly unlikely that a collision creates additional particles [2]. At this point the electromagnetic component will mostly ionize the surrounding air and start to die out.

[4]The atmospheric depth is usually given in g/cm^2.

To summarize, the amount of particles in an air shower will first start to increase. The growth of the amount of particles decreases as the energy per particle decreases. When the energy per particle falls below a threshold, no new particles are created and the remaining particles will decay. The atmospheric depth at which there is the most amount of particles is called X_{max}. This atmospheric depth X_{max} is an important characteristic of the air shower and is needed to determine the type of the initial particle [1]. Figure 2.3 gives a schematic picture of the amount of particles in an air shower as it propagates through the atmosphere.

2.2.2 Radio emission

A way to determine the shape of an air shower is by using radio signals [1]. As an air shower propagates through the atmosphere it emits radio waves. This is due to the acceleration of (newly created) charged particles in the air shower. There are two dominant mechanisms responsible for radio emission [5]. Both mechanisms lead to radio waves with coherent frequencies in the MHz regime, but with a different polarization [2]. Using the knowledge of these polarization patterns it is possible to reconstruct the air shower geometry [1]. The working principles of both mechanisms are schematically pictured in figure 2.4.

The main mechanism responsible for radio emission is the geomagnetic effect [5]. Due to the magnetic field of the Earth $\vec{B}$, negatively and positively charged particles are accelerated into opposite directions by the Lorentz force:

$$\vec{F} = q \cdot \vec{v} \times \vec{B} \tag{2.3}$$

where q is the charge of the particle, and $\vec{v}$ is the velocity of the particles in the air shower, which points roughly along the shower axis. Positively(negatively) charged particles are accelerated in the (-)$\vec{v} \times \vec{B}$ direction. This effectively constitutes a changing current in the $\vec{v} \times \vec{B}$ direction, which produces radio waves with a polarization along the $\vec{v} \times \vec{B}$ axis [5].

A secondary mechanism contributing to the generation of radio emission is the Askaryan mechanism [5]. As the air shower propagates through the atmosphere molecules are ionized during collisions. This frees electrons which travel together with the air shower, while the positively charged ions are left behind. This results in a negatively charged air shower front, leaving a positively charged region behind. This is effectively results in a changing current along the shower axis, which produces radio waves with a polarization pointing radially[5] towards to shower axis [5].

2.3 Indirect measurement of cosmic rays

UHECRs can be detected by measuring the radio emission of the air shower initiated by these particles. By combining a large number of radio antennas at different locations, it is possible to reconstruct the shower geometry [1]. The shower geometry leads to X_{max} and the incident direction of the cosmic ray. This is done by considering the polarization patterns of the different emission mechanisms and the changing speed of light in the atmosphere[6]. Furthermore, it is possible to determine the energy of the cosmic ray by measuring the energy in the radio emission. X_{max} is statistically dependent on

[5] in the plane perpendicular to the shower axis

[6] This is needed to translate time differences to path lengths.

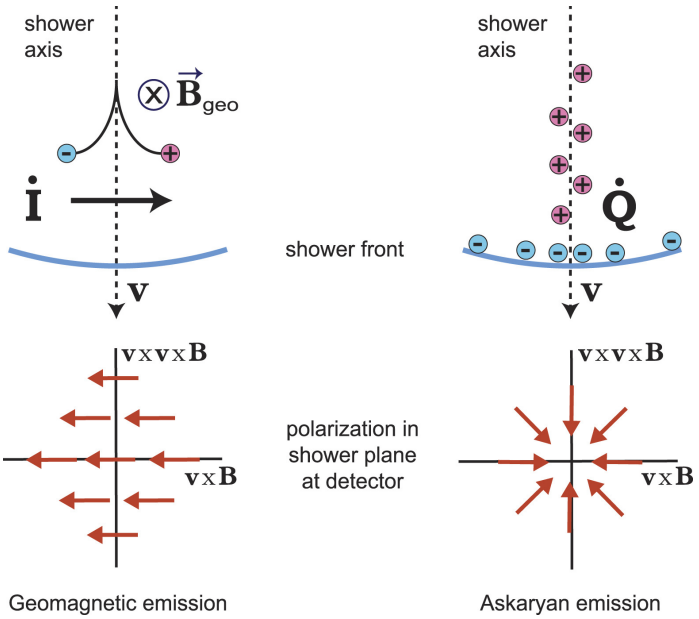

Figure 2.4: Schematic picture of the major mechanisms of radio emission [6].

the mass and the energy of the initial particle, by measuring the energy independently the mass can be retrieved [1]. This all leads to the type, incoming direction, and energy of the cosmic ray.

2.3.1 Giant Radio Array for Neutrino Detection

The Giant Radio Array for Neutrino Detection (GRAND) is a proposed project which aims to measure air showers indirectly initiated by neutrinos [1]. As a cosmic ray propagates through the cosmos, neutrinos and photons are created which travel in nearly the same direction. Since neutrinos undergo very little interaction, their path is almost a straight line, which means that they are more useful in determining the origin of UHECRs. These neutrinos can interact within the Earth's atmosphere, leading to the creation of their charged lepton counterpart. This lepton, for example a tau, initiates the air shower which will be measured using radio antennas. By measuring the air shower created by this tau, the energy, type and origin of the corresponding neutrino can be determined. Multiple events are needed to get accurate results, since there is some inaccuracy in every step needed to determine these factors.

To be able to record a large number of events, a huge detector is needed[7]. This is exactly why radio antennas are chosen: they are relatively cost friendly [1]. GRAND will be optimized for horizontal air showers[8]. The footprint of a horizontal air shower is bigger than that of a vertical shower. This means that the spacing between antennas can be reduced, while still measuring with the same number of antennas. Overall this means that with the same amount of antennas a larger area can be covered, leading to more documented events.

[7] GRAND will use 20 arrays of 10.000 radio antennas.
[8] Coming from zenith angles between 80°-90°.

3 Detection with radio antennas

Radio antennas are a valuable tool to detect cosmic rays. However, to understand the measured signal it is necessary to understand the main principles of antennas.

3.1 Antenna fundamentals

Most fundamentally, an antenna is a piece conducting material (e.g. copper wire) which reacts to a changing electromagnetic field [7]. By measuring the potential difference generated in the antenna, the effect of the external electromagnetic field can be measured. The measured potential difference V and incident electric field $\vec{E}_i$ depend on each other according to equation 3.1 [7].

$$V_A = \vec{h} \cdot \vec{E}_i \tag{3.1}$$

This relation is dependent on the vector effective length $\vec{h}(\phi, \theta)$, which is antenna specific and contains the so-called radiation pattern. This means that the measured potential difference depends both on the strength, and the polarization of the incident electromagnetic field at a given frequency. From this it also follows that the measured signal has the same frequency as the electromagnetic waves. Broadcasting and receiving are each other reciprocals. This means that an antenna behaves the same, whether broadcasting or receiving [8].

A common example of an antenna is the dipole antenna, see figure 3.1. This receiving(broadcasting) antenna consists of two arms which are connected by a unit capable of measuring(generating) a potential difference [7]. One arm of a dipole antenna is connected to the positive, while the other is connected to the negative of the measurement(generating) device. The polarization of electromagnetic waves generated by a straight-wire dipole antenna is along the same axis as the arms [7].

The efficiency of an antenna depends on its length compared to the wavelength of the electromagnetic waves. To have a decent efficiency in generating or detecting electromagnetic waves, the length of the antenna should be a decent fraction of the wavelength. In particular, for dipole antennas maximum efficiency is achieved for an arm length of $\frac{\lambda}{4}$ [7].

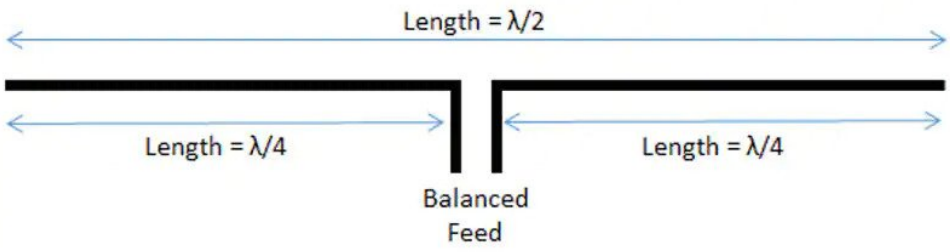

Figure 3.1: Schematic picture of a half-wave dipole antenna. One arm is connected to the positive, while the other is connected to the minus of the source. Figure from [9].

3.2 Reconstructing the electric field

In order to reconstruct the electric field from the measured potential it is necessary to know the radiation pattern of the antenna [7]. The radiation pattern represents the relative reaction of an antenna to electromagnetic waves coming from a direction (ϕ, θ). The radiation pattern can be determined by measuring the electric field at a number of points on a sphere around the antenna, or as in the case of GRAND it can be simulated [1, 8].

Since an antenna does not have perfect efficiency, it is necessary to incorporate this. The gain parameter combines the radiation pattern with the efficiency [7]. It relates the power of the electric field to the power of the current through the antenna. The efficiency of an antenna is dependent on the frequency, meaning that the gain is also dependent on the frequency. This means that the measured signal depends on the magnitude, polarization and frequency of the incoming electromagnetic waves. The gain is usually determined only in the far field approximation [7]. In general for the far field approximation to hold, the distance should be far greater than the wavelength of the electromagnetic waves: $r \gg \lambda$. Figure A.1 shows the gain parameter of the HORIZONANTENNA used in GRAND for two frequencies.

4 The GRAND antenna setup

In GRAND, air showers will be detected by measuring their radio emission. For this an antenna setup is in development. During the experiments discussed in this thesis, a prototype of this setup was used. The GRAND antenna setup will detect electromagnetic waves using the HORIZONANTENNA [1]. The signal generated in the antenna arms is transmitted to the *digitizer*. The digitizer is an electronics unit responsible for measuring, processing and communicating the signal. This will all be powered by a 12V battery charged by solar energy. A render of the prototype of the setup is shown in figure 4.1.

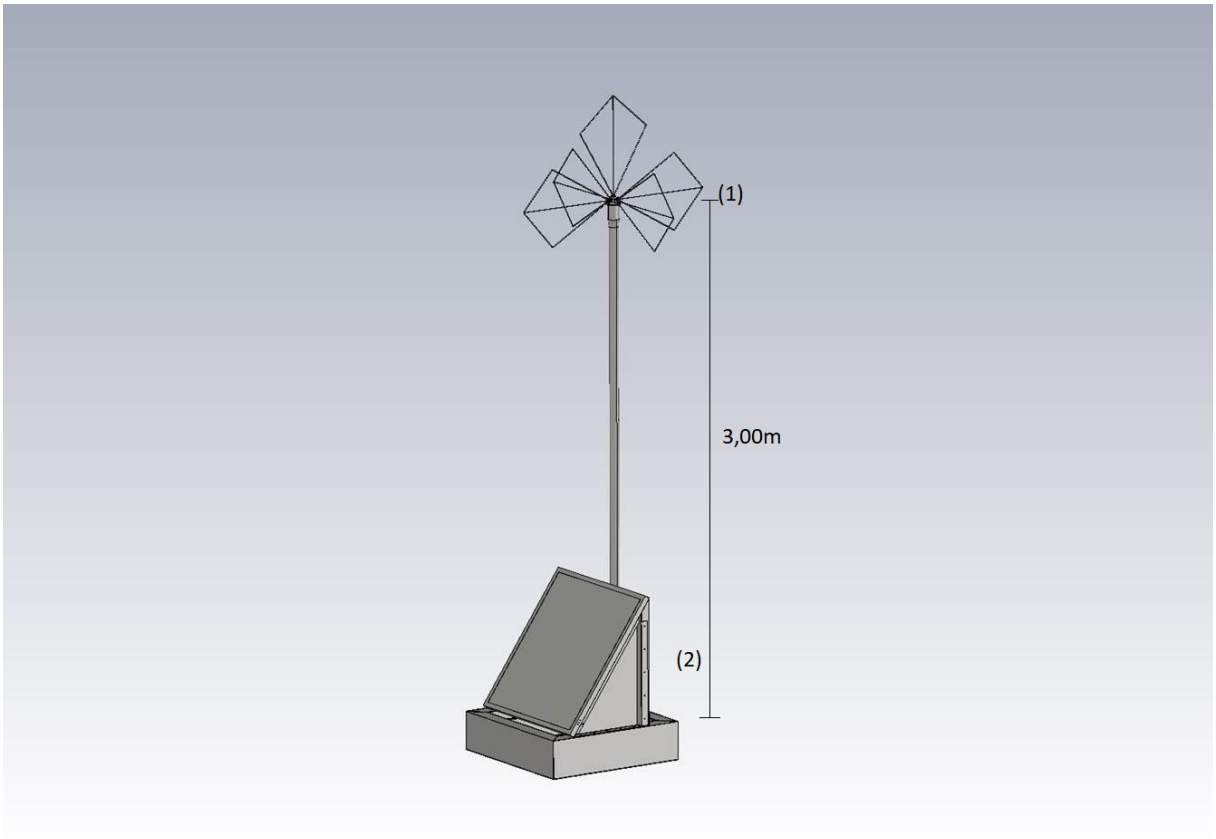

Figure 4.1: A render of the prototype of the GRAND antenna setup. (1): The HORIZONANTENNA*. (2) The antenna base, covered by a solar panel. The base contains a 12V battery and all the necessary digital equipment.*

4.1 HORIZONANTENNA

The HORIZONANTENNA is an active dipole antenna designed to work in the 50-200 MHz regime [1]. It is also called a bow-tie antenna, due to the shape of the antenna arms. The length of the antenna arms is chosen to be around $\frac{\lambda}{4}$ for the given frequency range. The HORIZONANTENNA consists of three independent antennas: 1 vertical monopole antenna (Z antenna), and 2 perpendicular dipole antennas in the horizontal plane (X & Y antenna). In principle, the gain of the two horizontal antennas is identical when rotated 90°. However, in reality they are not exactly identically due to external influences [8]. For example, solar panels near an antenna pointing to the south causes the north-south

antenna receptiveness to be different from that of the east-west antenna.

The antenna arms are attached to the so called *antenna nut*, see figure 4.2. In the prototype the nut is attached to a pole. In the antenna nut, the X, Y and Z arms are connected to their respective connectors. Using coaxial cables the antenna arms can be connected to the digitizer. Before the signal is transmitted to the digitizer, it is amplified by a low-noise amplifier (LNA) which is housed in the nut.

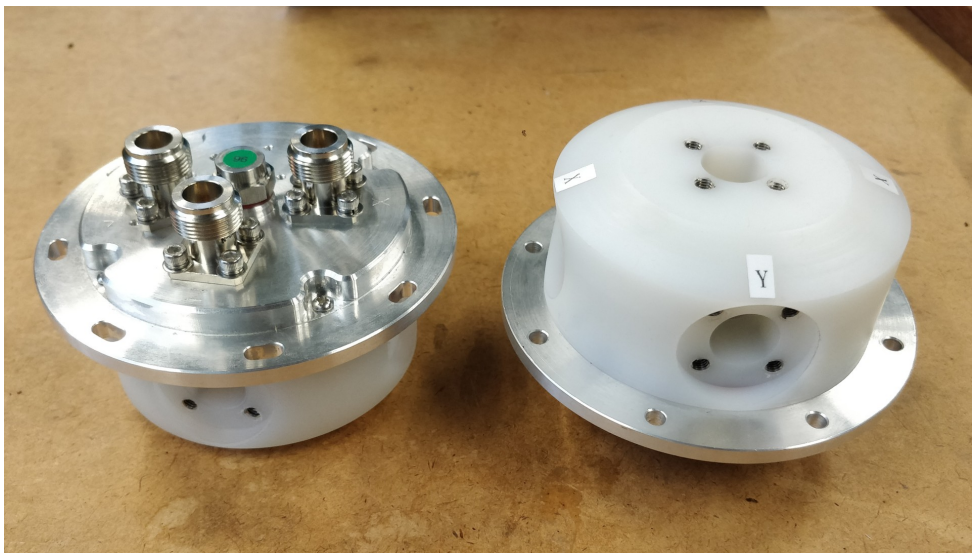

Figure 4.2: The antenna nut. Left: the 3 outgoing connectors on the bottom of the nut. Right: the 5 (2X, 2Y & 1Z) connectors for the antenna arms.

The HORIZONANTENNA is optimized for horizontal air showers. The antenna has a nearly flat response with respect to radio waves coming from low zenith angles [1]. This is shown by the gain plotted in figure A.1. Furthermore, the response to different frequencies in the 50-200 MHz regime is relatively flat [1].

4.2 Digitizer

The digitizer is the unit responsible for the actual data taking, see figure 4.3. It is an electronics board housed in a watertight Faraday cage. The antenna nut is connected to the connectors on the digitizer using coax cables. The digitizer measures the potential difference induced in the antenna arms. This is translated to a digital signal by a 14 bit 500 MHz analog to digital converter (ADC) [10]. Following the Nyquist sampling theory, the digitizer is capable of accurately measuring signals with a frequency between 0-250 MHz[9] [11]. Before the signal is transmitted to the ADC, it first passes through a 30-200 MHz filter ensuring the maximum frequency is not exceeded. The signal also passes another amplifier, as a result the signal can in total be amplified by a gain factor of [-14.0, 23.5] dB. The input range of the ADC is between -900 mV to +900 mV. The LNA in the nut and the amplifier on the board can be used to make sure the signal is in this range. The ADC produces some noise which is visible in the measurements. It is thus necessary to amplify a relatively low signal in order to make it visible

[9] In principle a different bandwidth could have been chosen, for more information see [11].

and/or improve the accuracy of the measurements. An over-saturated signal can be reduced to prevent clipping. Furthermore, a GPS sensor is connected to the board, which records the location and time. Some other sensors like a humidity sensor can also be connected to the board.

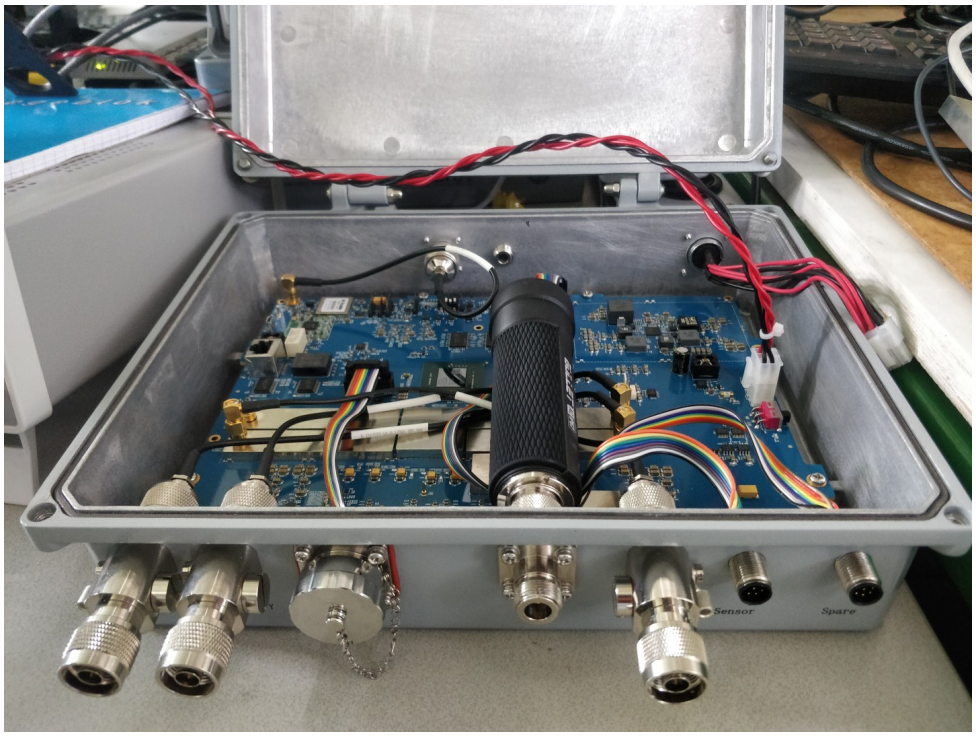

Figure 4.3: The current version of the digitizer. Ports from left to right: X-channel connector, Y-channel connector, Ethernet port, connector for external WiFi antenna, Z-channel connector, connector for sensors, spare connector. On the back of the housing there is a port for the power supply, and the GPS. The antenna ports are connected to their individual ADCs. The external WiFi antenna is connected to a bullet (the black cylinder), the unit responsible for establishing the mesh network.

4.3 Taking data

The recorded data is communicated over an Ethernet connection. Currently this can be either wired or wireless, but in the eventual setup it will be exclusively wireless. In the final version, each antenna setup will be connected to other nearby antennas to create a WiFi mesh network[10]. Using this mesh network, the antennas can communicate with each other which will be crucial for data logging. The digitizer continuously measures the voltage generated in the antenna arms. Whenever a trigger condition is met, this data is recorded as an event. Recorded events are transmitted to a computer, on which a data acquisition (DAQ) program runs.

The trigger conditions determine what kind of events are recorded. For example, you can record an event every 10 seconds to get some background measurements. More importantly when measuring

[10] A mesh network is a web of connections in which every station connects with other nearby stations. These stations pass through connections to other stations, essentially enabling communication between all stations in a mesh network.

air showers, you can record events when the measured signal obeys certain parameters. The parameters can be set to increase the probability that an event corresponds to a signal emitted by charged particles in an air shower. For example, the measured signal must be above some value, while being below the noise threshold for some time period before and after the signal. This describes a pulse-like signal, which is expected for an air shower. Recorded events of individual antennas are transmitted to a computer if their trigger conditions are met.

Presently, when multiple antennas are connected to the computer, the DAQ program filters events of different stations based on the time difference. This filters the events to those that could in principle correspond to the same source, since the time difference could be at most equal to the distance between the stations divided by the speed of light: $\Delta t = \frac{d}{c}$. Further reconstruction of the electromagnetic wave is needed to determine if this signal indeed corresponds to an air shower. Eventually, the setup will become autonomous. The antennas will communicate with each other to determine if the time difference between the events is sufficiently low.

5 Experimental goals

The original goal of my research was to measure air showers with a 5 antenna array, to be installed at the radio observatory in Nançay, France. This array was to be installed with my help around May, leaving time to analyse the measurements. Comparing the periodicity of the recorded events to the known period of the galactic background noise provides a way to test the setup[11]. Unfortunately, due to delays the installation of the array was pushed to early July, leaving too little time to fully analyze the measurements. However, some interesting experiments were performed beforehand to get accustomed to the equipment and its behaviour. These experiments and their results are discussed in the following sections.

First of all, measurements were taken in the lab. Secondly, the prototype discussed in section 4 was installed on the roof of the Huygensgebouw (Radboud University Nijmegen). Lastly, a three antenna array was installed in Nançay.

[11] The period of measured galactic noise should be equal to a sidereal day (23 hours and 56 minutes).

6 Experiments in the lab

Various measurements were performed in the lab to test the equipment, and as preparation for the installation on the roof and in Nançay. This allows to get accustomed to the equipment in a controlled environment. Furthermore, this gives an opportunity to determine some properties of the HORIZONANTENNA.

6.1 Setup: lab

In the lab of the High Energy Physics department (Huygensgebouw, Radboud University Nijmgen) the prototype was partially installed. The HORIZONANTENNA was placed on an elevation and connected to the digitizer powered by a 12V DC power supply. There were only 3 antenna arms connected due to limited availability. These 3 arms were connected to the X-channel and Z-channel. The Y channel was still connected to the empty nut.

To test the receiving characteristics of the GRAND antenna setup, a broadcasting antenna was used. This antenna consists of an approximately straight electrical wire connected to a function generator. This wire emits electromagnetic waves with the frequency of the input signal. The strength of the generated electric fields depends on the strength of the input signal and the gain of the wire. This signal is then detected with the HORIZONANTENNA. The length of the electrical wire was chosen to be $l = 70$ cm. This is about $\frac{\lambda}{4}$ for electromagnetic waves with a frequency of $f = 90$ MHz, which is well in the measurement regime. The electrical wire was connected to the source with a coax cable to reduce the emission of radio waves by this part. However, the end of the coax cable was open meaning that this part radiates with the same frequency as the main wire.

The polarization of the electromagnetic waves was changed by placing the broadcasting antenna in two orientations: vertical and horizontal. These orientations lead respectively to vertically and horizontally polarized electromagnetic waves. A schematic of the complete setup with the broadcasting antenna in vertical orientation is shown in figure 6.1. For completeness, a top-down view of the setup with the broadcasting antenna in horizontal orientation is shown in figure B.1.

6.2 Experimental method

To test the receiving characteristics of the HORIZONANTENNA, the setup described above was used. Using this setup it is possible to measure controllable man-made radio waves. Both the voltage and the frequency of the input signal of the broadcasting antenna were varied. Furthermore, the polarization of the generated radiation was changed. The input signal settings were changed in steps, the measurement of each specific setting ran for about 5-10 minutes. Every event was set to contain about 2 μs of data.

It was measured how the measured signal depends on the voltage through the broadcast antenna. To determine this dependence the measured signal was Fourier transformed, which was then averaged over all events. In order to pick out the contribution of the broadcast antenna to the signal, the amplitude of this Fourier transformation at the broadcasting frequency was used as a benchmark of the magnitude of the measured signal. This was done for both horizontal and vertical polarization,

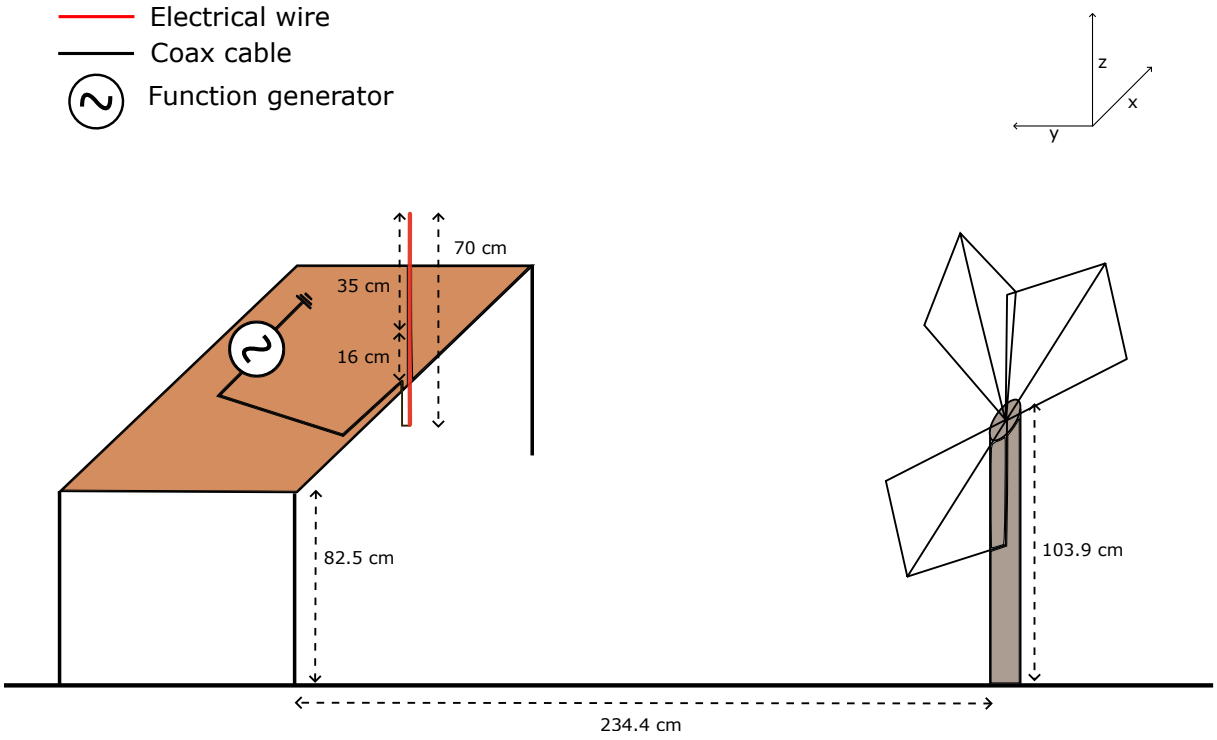

Figure 6.1: Schematic 3-dimensional picture of the setup used in the lab. Left: the broadcasting antenna, consisting of an electrical wire connected to a function generator using a coax cable, attached to a table in a vertical orientation. Right: The receiving HORIZONANTENNA. *Note: the* HORIZONANTENNA *was not actually supported by a pole, instead it was supported by two bricks on top of a table.*

for input voltages ranging between 2.0 Vpp and 5.0 Vpp at a broadcast frequency of 110 MHz.

An increase in the voltage through the broadcasting antenna should lead to a proportional increase in the magnitude of the emitted electromagnetic waves. This should in its turn lead to a proportional increase in the measured voltage through the receiving antenna. In short: a linear relation between the measured signal and the input voltage is expected in ideal circumstances.

It was also measured how the signal depends on the frequency of the signal through the broadcast antenna. This dependence is determined by the same way as above, only now with the broadcast frequency changing. This was done for both horizontal and vertical polarization, for broadcasting frequencies ranging between 70 MHz and 160 MHz, at a voltage of 2.5 Vpp.

The variation of the frequency gives an indication of how the gain of the HORIZONANTENNA changes as a function of frequency. The frequency dependence of the gain of the broadcasting antenna needs to be incorporated to correctly determine this effect.

6.3 Experimental results & discussion

6.3.1 Voltage dependence

The voltage dependence of the measured signal is determined by combining multiple measurements. One trace of those measurements, at an input signal of 5.0 V at 110MHz, is shown in figure 6.2. These measurements are then Fourier transformed and averaged. Two of those average Fourier transformations are given in figure 6.3. This figure shows the average Fourier transform of the measured signal for an input signal of 2.0 V and 5.0 V at 110 MHz. Plotting the amplitude at each voltage leads to voltage dependence shown in figure 6.4. Since in an ideal case there should be a linear relation between the measured signal and the voltage, a linear fit of the form $y = ax + b$ is performed where b corresponds to the background noise.

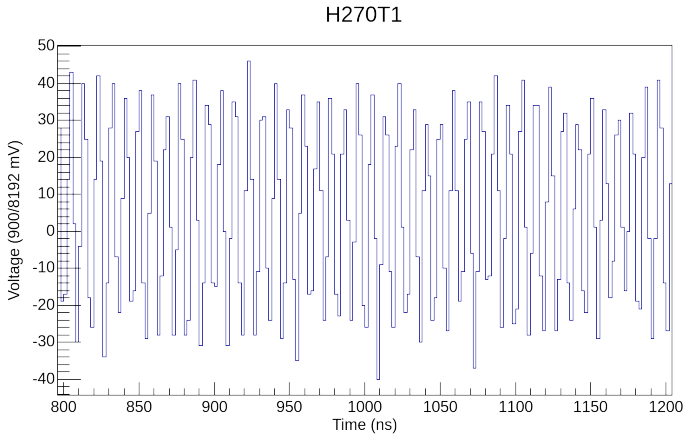

Figure 6.2: A zoomed in trace of the X-antenna for an input signal of 2.0 V at 110 MHz generating horizontally polarized waves.

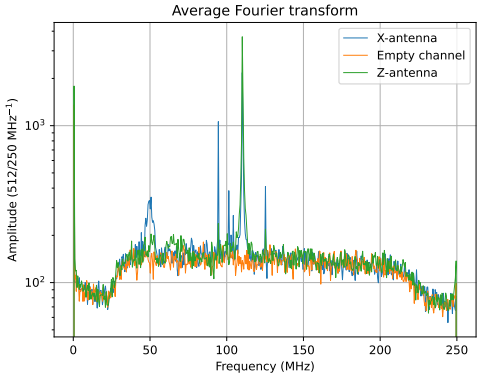

(a) Average Fourier transform for an input signal of 2.0 V at 110 MHz generating horizontally polarized waves.

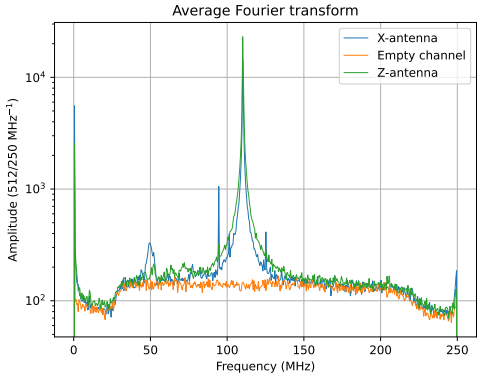

(b) Average Fourier transform for an input signal of 5.0 V at 110 MHz generating horizontally polarized waves.

Figure 6.3: Two average Fourier transforms.

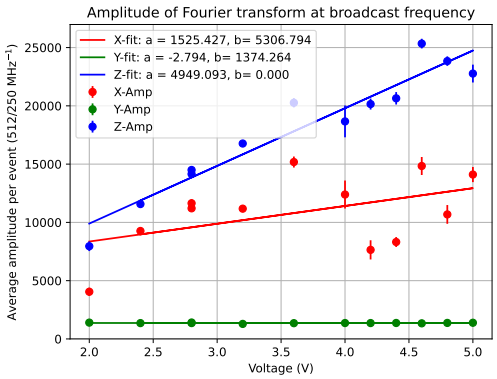

(a) Voltage dependence for horizontally polarized waves.

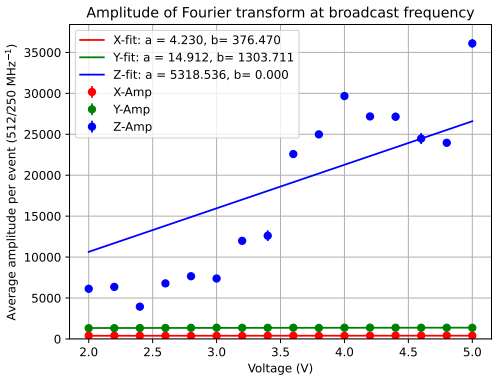

(b) Voltage dependence for vertically polarized waves.

Figure 6.4: Voltage dependence.

Figure 6.4a shows that for horizontally polarized waves, the Z amplitude follows more or less a straight line as expected. Furthermore, there is weak linear relation visible in the X amplitude. Lastly, the Y amplitude is close to a low constant as expected for an empty channel. The fact that these relations are not perfectly linear could have various reasons. For example, changing noise levels could influence the measurements. However, as shown in figure 6.3, the generated signal far exceeds the background noise in the lab, even for the weakest signal. This means that the noise level probably can't fully explain the fluctuations. Generally, since the measurements were taken in a lab, the circumstances were not ideal which could influence the measurements. The lower overall X amplitude compared to Z is a logical result of the orientation of the antenna arms. The X arms were rotated 90° around its axis and its zenith angle is turned 90° compared to the Z arms. As shown in figure A.1, this leads to a lower gain for the X arms. Moreover, this also causes the X antenna to be more influenced by small fluctuations.

Figure 6.4b shows that for vertically polarized waves, the measurements do not closely follow a straight line. The Z amplitude is on average slightly higher compared to the horizontal polarization, but there are more fluctuations. Furthermore, both the X and Y amplitudes are low and approximately constant. The relative difference of the Z amplitude compared to the X amplitude is far greater for vertical polarization compared to horizontal polarization. This is behavior that can be expected from the theory of a dipole antenna. In the ideal case of a straight-wire dipole, the polarization must be along the same axis as the wire to measure radiation with an acceptable efficiency. However, in the case of the X antenna, all parts of the antenna were perpendicular to the vertical polarization, meaning that it doesn't pick up a lot of signal. In the case of horizontal polarization, there is some overlap between the antenna wire and the polarization vector, resulting in bigger measurements. Similarly in the case of the Z-antenna, the antenna wire is mostly pointed in the vertical direction. As a result the measured amplitude is higher for vertically polarized waves. The large fluctuations of the Z amplitude is more difficult to explain, but once again the measurements were not taken in ideal circumstances.

The measurements were fitted to a function of the form $y = ax + b$, where b was required to be larger than 0 for physical reasons. In essence, b is just the noise level at the given frequency. This is something that was not taken into account directly. In further experiments the value of b should be deter-

mined by performing a noise measurement. Due to qualitative nature of the analysis performed, this does not pose a real problem in this case.

6.3.2 Frequency dependence

The frequency dependence of the measured signal is determined in the same way as described above, only now keeping the voltage constant while changing the frequency. Plotting the amplitude at each frequency leads to frequency dependence shown in figure 6.5.

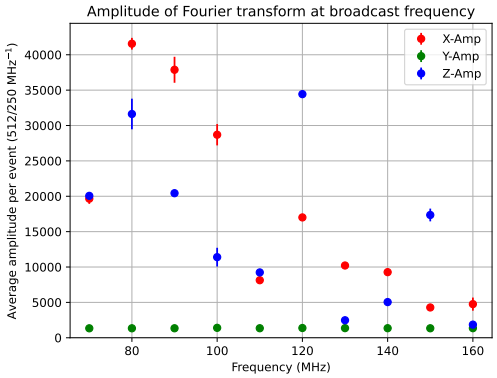

(a) Frequency dependence for horizontally polarized waves.

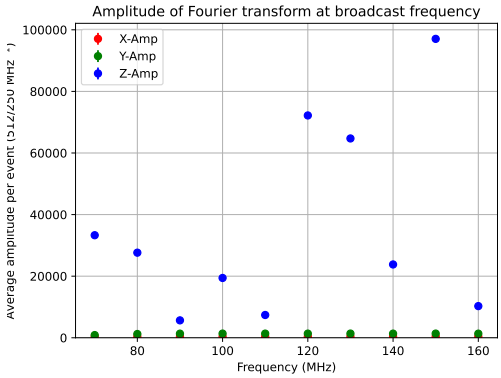

(b) Frequency dependence for vertically polarized waves.

Figure 6.5: Frequency dependence.

Both figures 6.5a and 6.5b show that there is only one relation visible. There is a downwards trend for the X amplitude in the horizontally polarized case. The Z amplitude fluctuates greatly for both horizontal and vertical polarization. As expected, the X amplitude is again on average lower in the case of vertical polarization compared to horizontal polarization. The amplitudes are subject to a lot more fluctuations from frequency to frequency. Even the relative difference between the amplitudes for horizontal polarization and the amplitudes for vertical polarization fluctuates largely. This is not something that can be explained by the theory behind a dipole antenna and/or the gain of the HORIZONANTENNA. For example, the difference between the amplitude for horizontal and vertical polarization at a frequency of 130 MHz is not something that is expected. Once again however, the measurements were taken in a lab in which a lot of reflecting material is present. The reflections on these metal objects interfere differently for different frequencies, which could explain the large fluctuations. To correctly determine the frequency dependence, the measurements should be redone in an empty radio-quiet environment. Secondly, the distance between the antennas should be increased sufficiently to ensure the application of the far field approximation.

6.4 Problems encountered

During the measurements various problems were encountered. An example of such a problem is given by the trace given in figure 6.6. The voltage suddenly exceeds the bounds of ±900 mV which is impossible. It is currently suspected that there is an error in reading out the data of long traces. This

was not observed for shorter measurement periods of approximately 2 μs. Another problem was the sudden oversaturation of the signal when using the same setup. The measured amplitude sometimes increased up to the maximum without adjusting the setup. This could be due to an error in setting the gain which was discovered in later stages, more about this in section 8. There might be other bugs in the software as well, results need to be analysed with care.

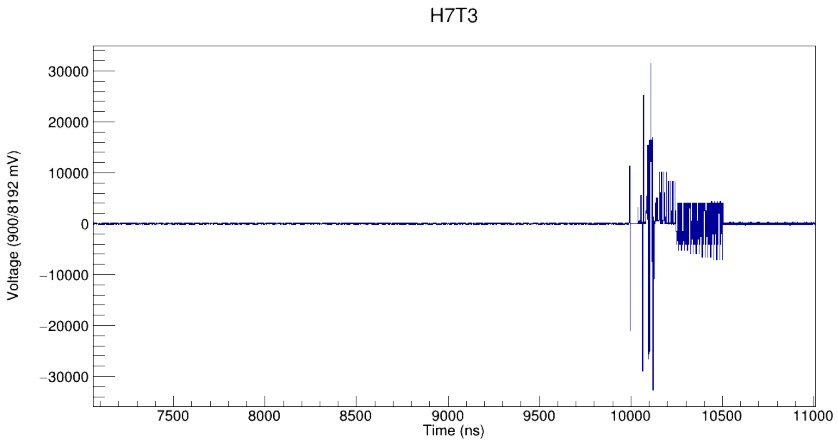

Figure 6.6: A trace of the Z channel containing unphysical results.

6.5 Conclusion

In conclusion, the antenna more or less behaves as expected. There was a more or less linear relation between the voltage and the measured amplitude. The amplitude changes with respect to polarization as expected from theory. The frequency behavior was not as expected, but this is likely due to the local environment of the antenna. To get a clearer view of the exact behavior of the antenna, further measurements in a more isolated environment need to be taken. Lastly, careful analysis is needed before making conclusions due to the current presence of software bugs and the problems in setting the gain.

7 Setting up the prototype on the roof

The prototype of the GRAND antenna setup as discussed in section 4 was installed on the roof of the Huygensgebouw (Radboud University Nijmegen), see figure 7.1. As in the setup in the lab, the X arms are rotated 90° compared to the discussed setup. As a result, these arms are more sensitive for radiation from the vertical direction.

Figure 7.1: The prototype of the GRAND antenna setup installed on the roof of the Huygensgebouw (Radboud University Nijmegen). The antenna at the base is used for establishing the WiFi mesh network.

Using this setup the noise spectrum given in figure 7.2 was measured over a time period of about 2 hours. The spectrum shows there is a lot of noise around the FM band[12] as expected. Especially large is the peak at 94.4 MHz, indicating there is some radio station nearby broadcasting at this frequency.

[12] 88-108 MHz

The X channel was oversaturated, consequently the spectrum of the X antenna is relatively flat. To get a more accurate result, the measurement should be redone with a lower gain on the X channel. However, it was not possible to redo the measurement in time due to several reasons. Firstly, the 12V battery connected to the solar panel depleted quickly. This was consequently replaced by a 12V power supply, but due to the closed enclosure and the sun the components got very hot. As a result a hardware failure occurred after the initial run of two hours. After this was repaired, no stable power supply could be achieved due to heating issues. In the end there was not enough time to redo the measurements due to these issues. These heat problems need to be resolved for the definitive setup.

Some other characteristics of the setup are also visible in the noise spectrum. First of all, there is a direct current going through all channels which is visible as the peak at 0 MHz. Secondly, the channel only connected to an empty nut measured more than the channel supposedly connected to the Z arms. Also, in contrary to previous measurements the X-antenna measured the biggest signal. This does not agree with the results discussed in section 6.3. A man-made signal usually has a horizontal propagation direction which allows this comparison. The cables probably got accidentally switched around during the installation. Furthermore, the Z spectrum nicely shows the shape of the frequency filter present in the digitizer. Lastly, the peaks in the Z spectrum also shows that either the metal in the antenna nut actually also picked up some of the signal, or there is some signal leaking between the ADC channels.

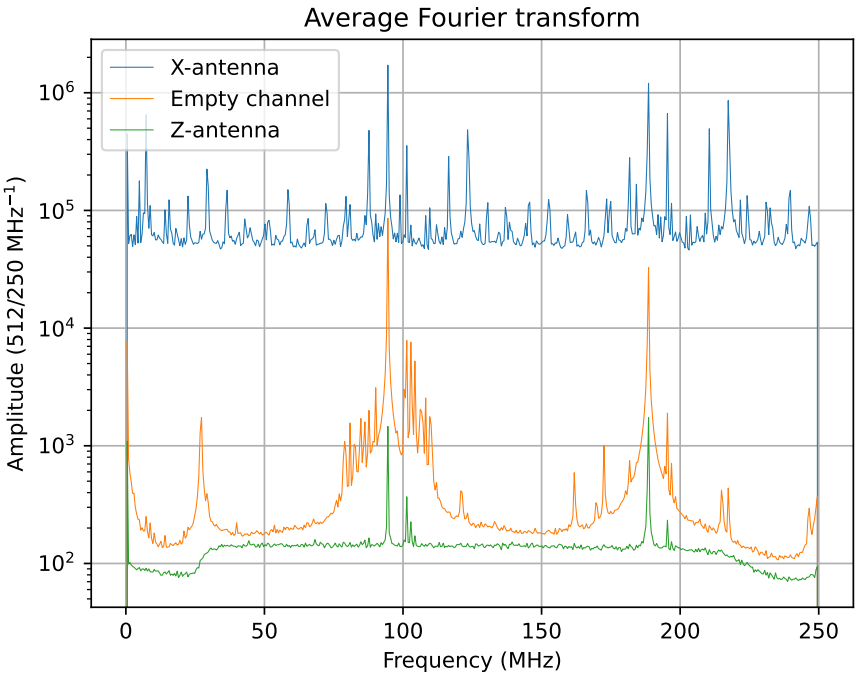

Figure 7.2: The noise spectrum in Nijmegen. Note: The channels are likely switched around. The X channel was oversaturated, resulting in a relatively flat spectrum.

8 Small array in Nançay, France

At the Nançay radio observatory in France a total of 3 antennas were installed. The essential components are the same as that of the setup discussed in section 4. The key differences are:

- An FM filter[13] was added, filtering the signal before it is passed through to the ADC.
- It is powered by a DC power supply.
- For some stations a fiber connection was used.
- The base is improvised out of a combination of a parasol base and PVC tubes.

There was also a problem with the conduction between the antenna arms and the antenna nut due to mismatching parts. This was solved by putting some aluminum foil between the antenna arms and the nut. Two of the antennas are visible in figure 8.1.

Figure 8.1: Picture of the antenna setup as used in Nançay.

The setup was tested to determine if the setup worked correctly and to fine tune the trigger settings. First the background noise was measured overnight with 1 antenna, see figure 8.2. While the data logging worked as it should, it also showed that only the Z-antenna effective picked up a signal. This indicates that the measured signal of the X- & Y-antennas is comparable in magnitude to the ADC noise. To solve this the gain needs to be increased, which was then quickly discovered to not work as expected. This is a problem that needs to be resolved. It was traced to the hardware initialization, which requires a high enough voltage setting to properly configure the flash ADC and the amplification on board. The amplitude of the Z-antenna also nicely shows the effect of the used FM filter,

[13] Blocking frequencies from 88-108 MHz.

visible as an abrupt dip at the start of the FM regime. It was also tested if the DAQ could successfully combine events of multiple stations. This appeared to work as it should, except for some instability issues probably caused by the used fiber connection. These gain and instability issues need to solved, after which it will become possible to measure the first air showers!

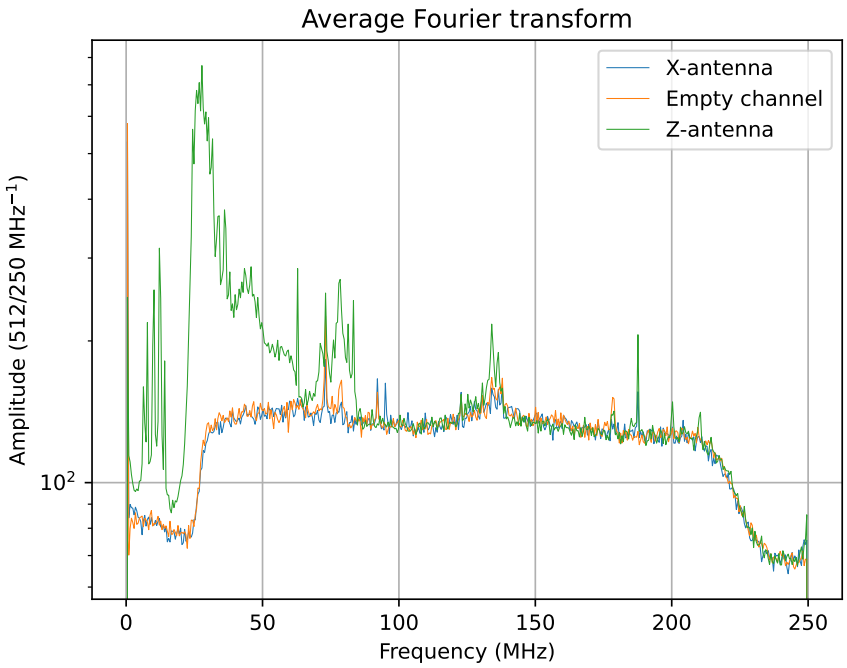

Figure 8.2: An overnight measurement of the noise spectrum in Nançay.

9 Conclusion

The prototype of the GRAND antenna setup behaves as expected, but there is still room for improvement. Software and hardware problems present in the DAQ and digitizer need to be solved. Furthermore, heat and instability issues need to be resolved. The measurement of air showers with larger arrays will undoubtedly point out more room for improvement, but the prototype provides a nice start for measuring air showers.

References

[1] GRAND Collaboration, "Giant radio array for neutrino detection: science and design", (2019).

[2] S. Jansen, "Radio for the masses" (Apr. 2016).

[3] E. M. Holt, "Combined detection of muons and radio emission of cosmic-ray air showers" (Apr. 2018).

[4] A. Escudie et al., "Radio detection of atmospheric air showers of particles", 10.48550/ARXIV.1903.02889 (2019).

[5] J. Alvarez-Muñiz et al., "Radio pulses from ultra-high energy atmospheric showers as the superposition of Askaryan and geomagnetic mechanisms", Astropart. Phys. **59**, 29–38 (2014).

[6] F. G. Schröder, "Radio detection of cosmic-ray air showers and high-energy neutrinos", Progress in Particle and Nuclear Physics **93**, 1–68 (2017).

[7] W. L. Stutzman and G. A. Thiele, *Antenna theory and design* (Wiley, 2013).

[8] A. W. Rudge et al., *The handbook of antenna design* (Peregrinus on behalf of the Institution of Electrical Engineers, 1983).

[9] https://www.digikey.com/en/blog/use-traps-to-enable-multiband-operation-with-dipole-antennas.

[10] T. Wijnen, "The grand digitizer (preliminary)", Radboud University (unpublished) (2022).

[11] R. G. Lyons, *Understanding digital signal processing* (Addison-Wesley, 1996).

A Gain HORIZONANTENNA

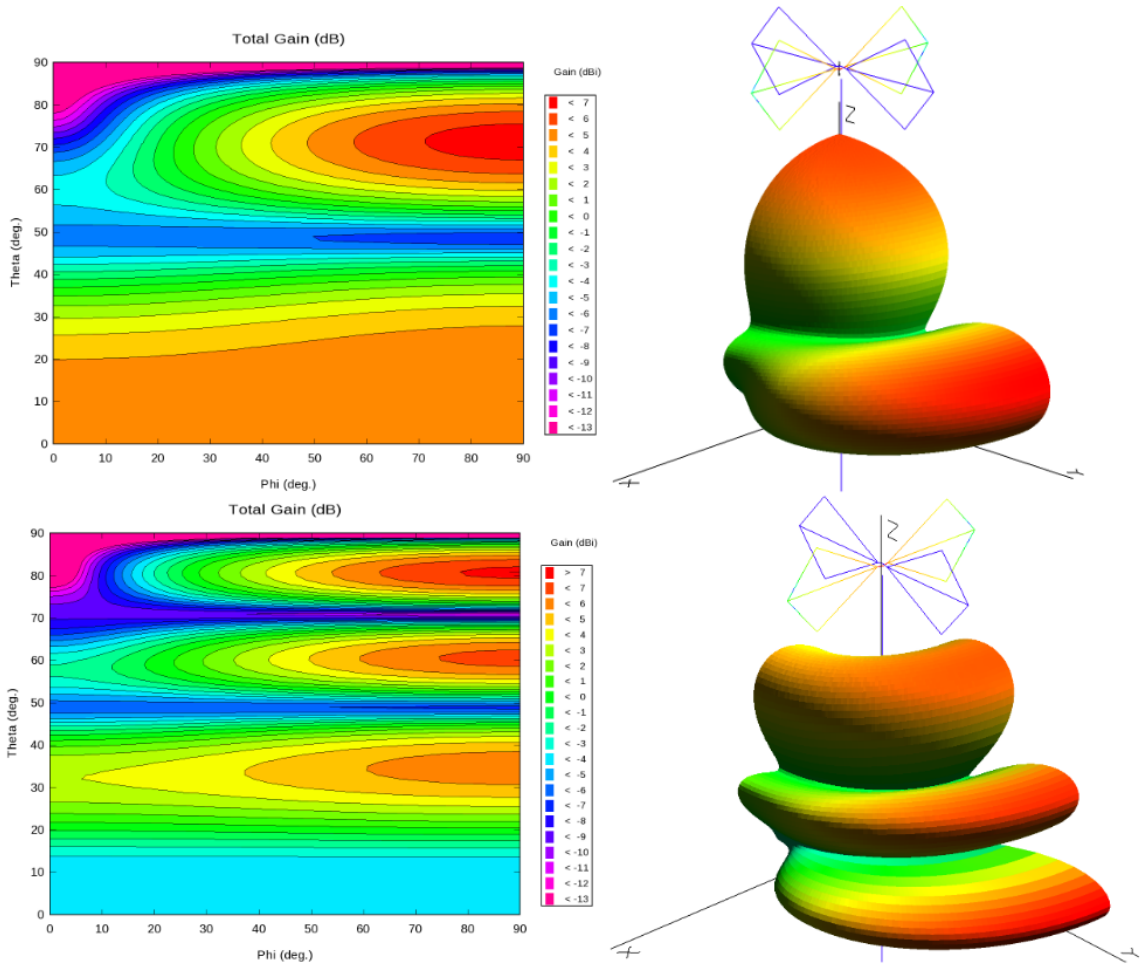

Figure A.1: Total gain of the X-arm of the GRAND HORIZONANTENNA *as a function of direction. Top: 50 MHz. Bottom: 100 MHz. Computed by the NEC4 simulation code. The simulation is not accurate for high zenith angles due to simplifications [1].*

B Schematic setup: lab

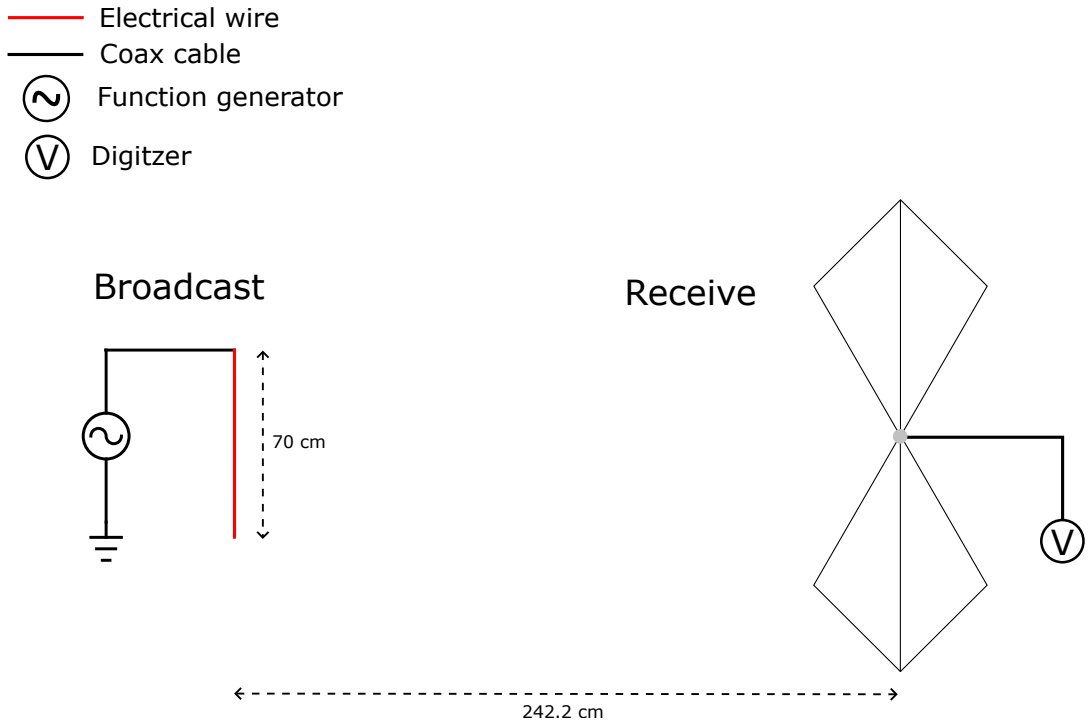

Figure B.1: Schematic top-down view of the setup used in the lab. Left: the broadcasting antenna, consisting of an electrical wire connected to a function generator, on a table in a horizontal orientation. The broadcasting antenna is positioned on a height of $h = 84.7cm$*. Right: The receiving* HORIZONANTENNA*. The receiving antenna is positioned on a height of* $h = 103.9cm$